CROSS-STREAM EVOLUTION OF THE FREE SHEAR LAYER BEHIND A WING

Muhammad Omar Memon
Department of Mechanical and Aerospace Engineering
University of Dayton
300 College Park, Dayton, Ohio 45409
mmemon1@udayton.edu

Aaron Altman
Department of Mechanical and Aerospace Engineering
University of Dayton
300 College Park, Dayton, Ohio 45409
aaltman1@udayton.edu

ABSTRACT

The free shear layer in the wake behind a wing has revealed some surprising results in the evolution of the cross-stream in both the magnitude and direction of the flow. Cross-stream planes were interrogated using Particle Image Velocimetry (PIV) in the UD Low Speed Wind Tunnel three chord lengths downstream of an AR 6 wing with a Clark-Y airfoil. The velocity components in the cross-stream plane indicate significant changes in the direction of the flow in the wake free shear layer corresponding to the upper and lower surfaces of the wing. There was minimal cross flow in the free shear layer at low angles of attack indicating quasi-two-dimensional flow in the streamwise direction. Shear was established in the cross flow direction as the angle of attack increased. Flow corresponding to the upper portion of the stratified wake was in an inboard direction towards the root. Flow corresponding to the lower portion of the stratified wake was outboard towards the tip and wingtip vortex. The transition between the quasi-two-dimensional wake and established cross-flow in the free shear layer happens in the vicinity of the maximum lift to drag ratio (max L/D) angle of attack.

INTRODUCTION

Several chord lengths distance downstream of a wing, the so-called fully rolled up wing wake evolves into a discrete wingtip vortex pair and a free shear layer. While the wingtip vortices embody a large portion of the total drag at high lift angles, flow properties in the free shear layer also reveal its contribution to the aerodynamic efficiency of the aircraft as an analogue for parasite drag. Since aircraft rarely cruise at maximum lift to drag ratio conditions (because it is generally too slow), the fluid dynamic analogy for the balance between the lift induced drag and the parasite drag can be explored by studying the interaction between the wingtip vortex and the free shear layer.

The relationship between the lift induced drag (contribution from the wingtip vortex) and the profile drag (contribution from the free shear layer) was related in terms of the axial core velocity by a number of researchers (Batchelor, 1964; Brown, 1973; and Memon & Altman, 2015). Batchelor (1964) presented a relationship between the azimuthal velocity and the core axial velocity of the wingtip vortex. Viscous effects in the wing wake reduce the azimuthal velocity (mostly of the outer core) resulting in the loss of axial momentum in the wingtip vortex core. Brown coupled the axial core velocity to the relationship between the profile drag and the lift induced drag. He found that the vortex axial core flow formed at the vortex center may exhibit wake-like (less-than the freestream) or jet-like (greater-than the freestream) tendencies depending on the ratio of profile drag to the induced drag for a given lifting surface. Several experiments have shown similar results [Chow et al. (1997), Lee and Pereira (2010), etc]. Memon & Altman (2016) investigated the wingtip vortex roll up process as a function of angle of attack three chord lengths downstream of a Clark-Y wing. The authors found a discontinuity in the behavior of the vortex in terms of vorticity and dissipation (exergy) around max (L/D) angles of attack. The discontinuity was attributed to the transformation of the wingtip vortex core axial flow from wake-like to jet-like around those angles of attack.

Wygnanski et al. (1986) showed that the free shear layer wake is unique and changes as a function of the drag coefficient of the turbulence generator as well as several other factors. Gunasekaran & Altman (2016) explored the turbulence character in the wake of a flat plate in the mid semi span free shear layer and showed that the free shear layer moves below the wingtip vortex with increasing angle of attack. The wingtip vortex remained independent of the free shear layer at higher angles indicating a transfer of momentum from the free shear layer to the wingtip vortex at small angles of attack.

EXPERIMENTAL SETUP

The experiments are conducted in the University of Dayton Low Speed (in Open Jet mode) Wind Tunnel with a test section cross-section of 30 *in* x 30 *in*. (812 *mm* x 812 *mm*). The tunnel inlet includes 6 anti-turbulence screens and has a contraction ratio of 16:1. The semi-span wing of semi-span AR = 3 comprising a Clark-Y airfoil was mounted vertically on a Griffin Motion SN: 1651 rotary stage to ensure precise angle-of-attack increments of 1° and accuracy within several arc-seconds. A Quantel 200

mJ/pulse laser (Twins) was used to create a light sheet in the cross-stream plane. The laser beam was expanded into a sheet of approximately 9 *mm* thickness. A PCO 1600 camera with a 180 *mm* lens was used. The field of view (FOV) was 88 *mm* x 66 *mm* and was subdivided into correlation windows in a two-pass 64 pixel/32 pixel interrogation region size with a 50% overlap. This yielded an overall resolution of 17.3 vectors per millimeter. The data was taken three chord lengths downstream of the trailing edge of the Clark-Y wing across a range of angles of attack. Representative time between laser pulses (Δt) for the experiments range from 140 to 220 microseconds. A pulse generator from Quantum Composer (Model 9614) was used to synchronize the time between laser pulses with the PCO 1600 camera shutter. The uncertainty of 5 ns and 0.1 m/s was used for Δt and freestream velocity respectively (Memon & Altman, 2015). The number of image pairs recorded varied between 3000 and 6000. Image cross-correlation was performed using DPIV from ISSI. Figure 1 shows the wind tunnel test section with the semi-span wing installed. The schematic of the PIV setup with the axis system definition is shown in Figure 2.

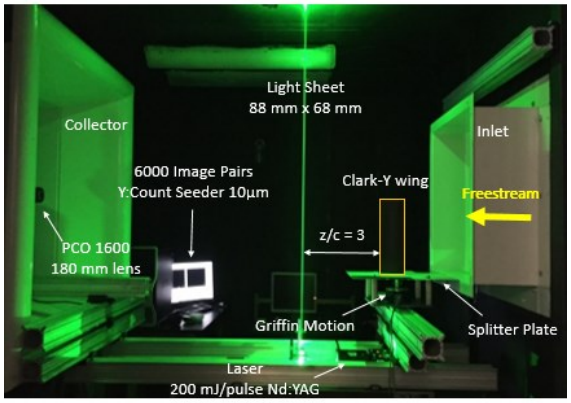

Figure 1. Test section with half wing installed.

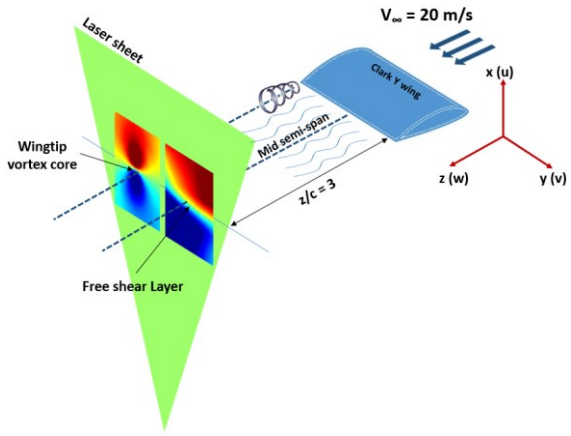

Figure 2. Schematic of the PIV setup with the axis system.

WINGTIP VORTEX RESULTS

In order to understand the effects of free shear layer contributions to the wingtip vortex, three angles of attack were tested at the same freestream as the free shear layer data acquired previously. Only three angles are shown here as the most representative results; a zero lift angle (-3°), 0° angle where the wingtip vortex is supposed to be fully formed, and a higher angle (6°) where a much larger absolute physical scale vortex is expected. Figure 3 shows the v component velocity contours for each of the three angles of attack tested. The contour for the -3° case is on a different contour scale (to enable visibility) whereas the 0° and 6° contours share the same contour scale (on the far right). It is visible that the vortex core is not developed at the zero-lift angle (-3°). However, at higher (positive) angles, the vortex inner core is fully developed and the size of the vortex grows linearly as a function of angle of attack.

Figure 4 shows the v component velocity profiles for each angle of attack in terms of the absolute magnitudes and also normalized by the v velocity peaks. For the -3° case, there is much asymmetry observed in the area that is comprised of the feeding shear layer. Since there is nearly zero lift produced at -3°, the flow is dominated by the parasite drag. Very little or no asymmetry is observed in the u velocity profiles for the 0° and 6° angles of attack. Large differences exist between the -3° angle and the other angles. This is evidenced in the normalized profiles in Figure 4.

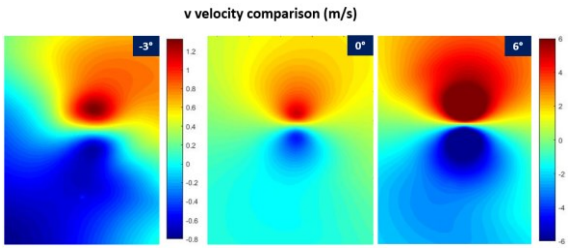

Figure 3. v velocity evolution showing vortex core is not developed at -3° (zero lift angle), fully developed vortex core beyond 0° angle of attack

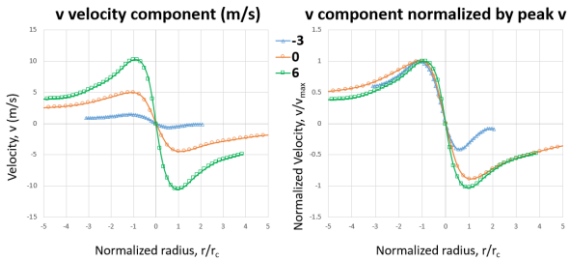

Figure 4. Left: v velocity profile comparison showing asymmetry for -3° and symmetric behavior for 0° and 6° angle of attack. Right: v velocity profiles normalized by the peak v showing large difference for -3° angle of attack

It is noteworthy that the -3° case resembles pure shear compared to the other positive (0° and 6°) angle of attack cases. In order to better visualize it, the rotation field in the v-velocity component in the -3° case is subtracted and compared to the velocity field obtained from the mid semi-span free shear layer in the wake. Figure 5 compares the velocity components contributing to pure shear in the wingtip vortex and the mid semi-span free shear layer.

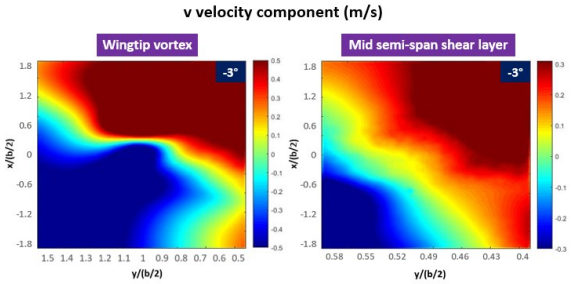

Figure 5. v-velocity component contours contributing to the isolated shear shows similarities to the wingtip vortex and the mid semi-span free shear layer for the -3° case.

The development and evolution of the wingtip vortex is clearly seen in the vorticity contours in Figure 6. The contour for the -3° case is on a different contour scale whereas the 0° and 6° contours share the same contour scale (on the far right). The magnitudes of the vorticity profiles seen in Figure 5 show that the vortex core is not fully developed at the -3° angle. The difference in shape in the normalized -3° plot is evidence of that behavior. The vortex is fully developed at 0° angle of attack as seen from the contour in Figure 5 and consequent profiles in Figure 6.

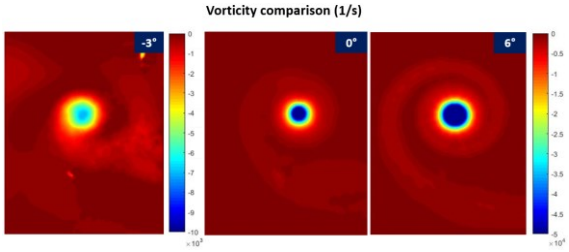

Figure 5. Velocity evolution showing development of the vortex core as a function of angle of attack.

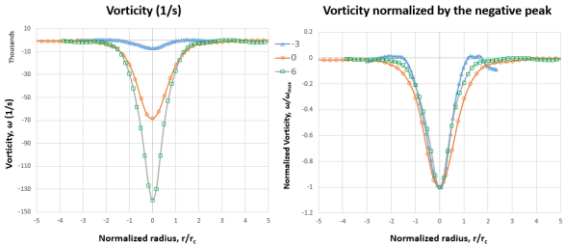

Figure 6. Left: Comparison of the vorticity profiles showing gradual increase in magnitude with angle of attack. Right: vorticity profiles normalized by negative peak vorticity showing large differences in the shape of the inner core boundary for each angle of attack

The second derivative (dissipation) quantity exergy shows similar behavior in Figures 7 and 8. The contour for the -3° case is on a different contour scale whereas the 0° and 6° contours share the same contour scale (on the far right). While the -3° angle shows highly asymmetric behavior, little asymmetry is observed for the 0° case in the absolute magnitude exergy profiles in Figure 8. The exergy destruction rate highlights small differences in such quantities.

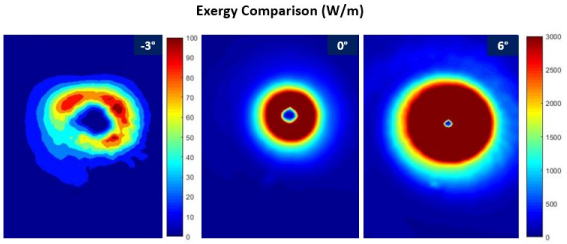

Figure 7. Exergy evolution showing development of the vortex core as a function of angle of attack.

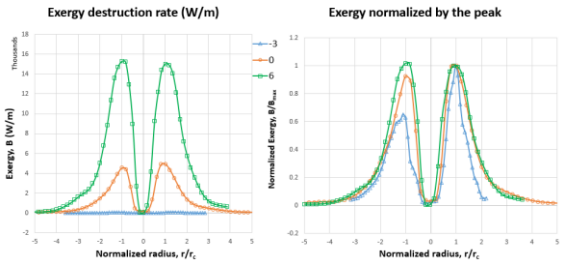

Figure 8. Left: Exergy profile comparison showing gradual increase in the magnitude with angle of attack. Right: exergy profiles normalized by the peak exergy showing large differences in the inner core boundary for -3° angle of attack.

FREE SHEAR LAYER RESULTS

For the free shear layer, the u (downwash) velocity component contours for each of the representative angles included here are shown in Figure 9. The magnitude of the downwash velocity increases with increasing angle of attack as expected. Figure 10 shows selected sectional profiles of the u (downwash) velocity component for each angle of attack. The arrow shows the direction of the increase in magnitude for a set of angles of attack. The u velocity component plot shows (negative) increase in the magnitude with increasing angle of attack. The shape of the profiles starts to change at positive angles of attack (from 0° to 3°) and progresses to become much more significant at higher angle (6°). It is also noteworthy that the u velocity component is symmetric on either side of the free shear layer for the 6° angle. This behavior could be indicative of the total segregation of the free shear layer from the wingtip vortex at higher angles. In Figure 11 the downwash component is normalized by the peak (hump) indicating similarity in shape from 3° up to 6° angle of attack. Also curious is that the downwash associated with the lower surface varies much less as a function of angle of attack as the downwash associated with the wing upper surface.

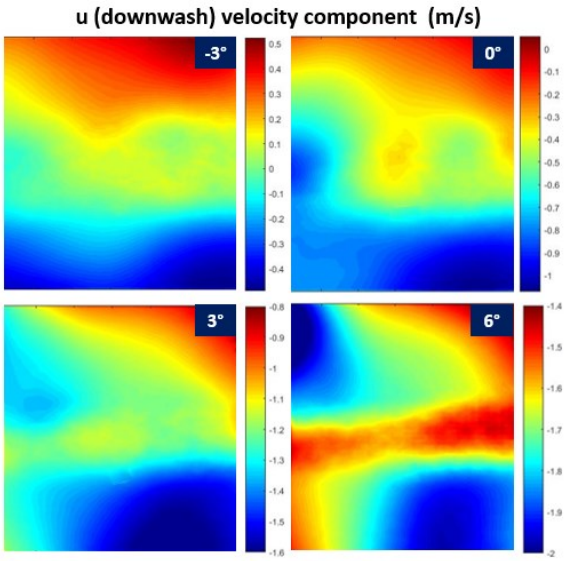

Figure 9. u (downwash) velocity distribution contours for various angles of attack showing increase in the downwash with increasing angle of attack.

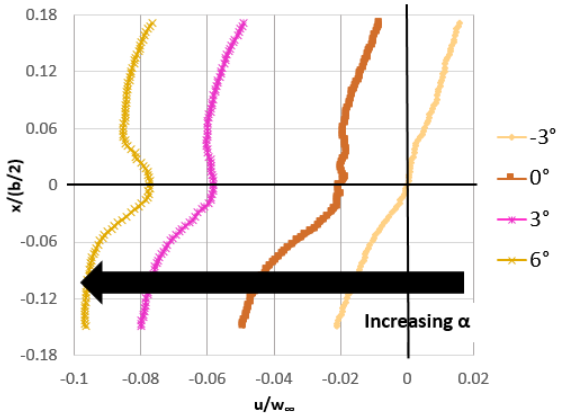

Figure 10. u (downwash) velocity component profiles showing linear (negative) increase in the magnitude with angle of attack. Noticeable changes in the profile shapes are seen at 0° up to 3° before a more consistent shape is seen at 6° angle of attack.

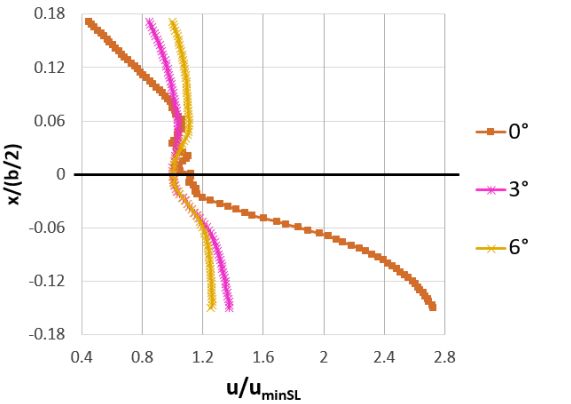

Figure 11. u (downwash) velocity component profiles normalized by u-minimum showing distinct changes in 0° angle of attack profile in an otherwise consistent behavior across other angles of attack.

The v (spanwise) velocity component contours are shown in Figure 12. From -3° up to 0° angle of attack, no distinct shear layer can be discerned. From 0° to 3° angle of attack, spanwise flow in the free shear layer is beginning to develop however is not yet uniform across the span (within the wake). Beyond 3° angle of attack (6°), a uniform topology is formed in the shear layer across the span. Figure 13 shows selected sectional v component profiles for each angle of attack. The arrow shows the direction of the increase in magnitude for a set of angles of attack. The results are intriguing where the (negative) magnitude increases only in the portion of the stratified free shear layer originating from the upper wing surface with increasing angle of attack (from 0° to 6°). The contribution from the lower surface is relatively constant. Figure 14 shows peak normalized v component profiles. The results are only plotted for 0° to 6° angle of attack for visual clarity. The 0° case is different compared to the other cases where the shear layer is mostly uniform. This behavior could be interpreted as evidence of increasing velocity transfer from outboard (wingtip) to inboard (mid semi-span) with increasing angle of attack.

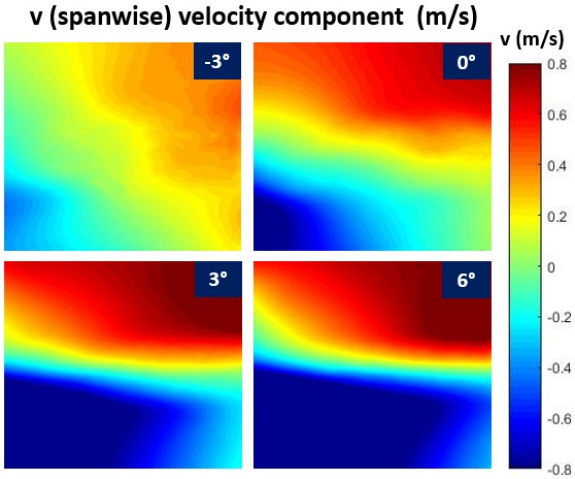

Figure 12. v (spanwise) velocity distribution contours for various angles of attack showing velocity in opposing sense for each of the angle of attack.

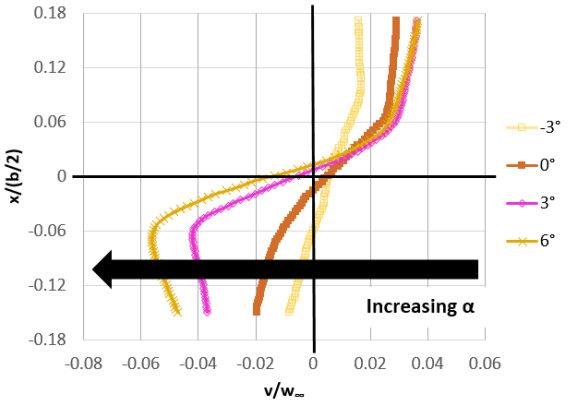

Figure 13. Cross-sectional lines through the v component velocity contours showing gradual increase in the v component (in the lower surface of the wing) with increasing angle of attack.

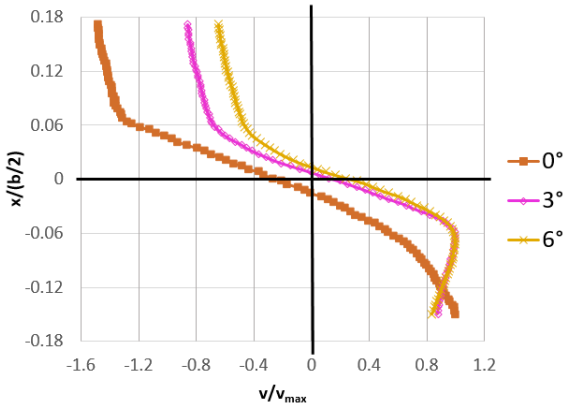

Figure 14. v (spanwise) velocity component normalized by the peak showing distinct changes in 0° angle of attack profiles in an otherwise consistent behavior across other angles of attack.

To verify whether or not there is actually a net flow moving from inboard to outboard and vice versa, vector plots were used to highlight the direction of the flow. Figure 15 shows velocity vector plots for each of the four (2°, 4°, 6° and 8°) angles of attack. The u velocity component shows the mean flow occurring in the downward direction as would be expected due to downwash in the cases of positive lift. The v velocity component shows flow in opposite directions in the stratified shear layer resulting from the upper and lower surface flow in the wake of the wing. Figure 15 illustrates the vectors resulting from the upper and lower surface flows of the wing along with the location of the wing root and tip upstream. As seen from the pressure side of the wing (annotated in green squares), the magnitude and direction of the velocity vectors are relatively constant with increasing angle of attack. This shows that the change in the lower surface wing wake do not contribute to transfer of momentum from the free shear layer to the wingtip vortex. On the other hand, the magnitude and direction of the velocity vectors change significantly on the upper surface side of the wing wake as a function of angle of attack, as shown in the red circles in Figure 15. When obtaining the net contribution of the wing wake downstream in the crossflow, there is a net momentum transfer from inboard (from the wing root) to outboard (towards the wingtip). Similar behavior was evident in the streamwise flow of a flat plate in a recent research (Gunasekaran & Altman, 2016). It is worth noting that despite much smaller velocity magnitudes in the cross flow compared to the streamwise flow, the net transfer of momentum from inboard to outboard can still be observed. This momentum transfer is responsible, at least in part, for altering the balance between the parasite drag and the lift induced drag. It is also noted that this transfer of momentum occurs in the vicinity of maximum lift to drag ratio angles of attack.

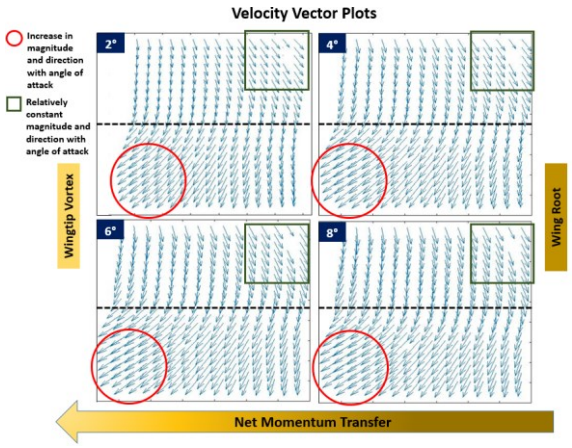

Figure 15. Velocity vector plots for each angle of attack showing significant changes (red circles) in the stratified wake of the upper surface of the wing and relatively constant behavior (green squares) in the lower surface wake of the wing.

CONCLUSIONS

Velocity components in and around the stratified free shear layer in a wing wake showed counter flow presumably corresponding to behavior associated with the upper and lower surfaces of the wing. This behavior indicated the possibility of the transfer of momentum (from inboard to outboard of the wing). The transfer of momentum supports the concept behind the analogy for the balance between parasite and lift induced drag. Results were also indicative of the segregation of the free shear layer from the wingtip vortex at higher angles of attack. The transition from minimal cross flow in the free shear layer to the well-defined uniform shear in the cross flow direction occurs in the vicinity of the maximum lift to drag ratio (max L/D) angle of attack.

REFERENCES

Batchelor, G. K. (1964). Axial flow in trailing line vortices. *Journal of Fluid Mechanics*, 20, pp 645- 658

Brown, C. E., "Aerodynamics of Wake Vortices," *AIAA Journal*, Vol. 11, No. 4, pp. 531–536, 1973.

Chow, J., G. Zilliac, and P. Bradshaw, "Turbulence Measurements in the Near Field of a Wingtip Vortex", *NASA-TM 110418*, 1997.

Gunasekaran, S., Altman, A., "Is there a relationship between the turbulence character of free shear layer and the wingtip vortex?" *54th Aerospace Sciences Meeting and Exhibit*, January, 2016, San Diego, CA.

Lee, T., and Pereira, J., "Nature of Wakelike and Jetlike Axial Tip Vortex Flows," *Journal of Aircraft*, Vol. 47, No. 6, November–December 2010.

Memon, M. O., Wabick, K., Altman, A., Buffo, R., "Wing Tip Vortices from an Exergy-Based Perspective", *Journal of Aircraft*, Vol. 52, Special Section on Second High Lift Prediction Workshop (2015), pp. 1267-1276. doi: 10.2514/1.C032854.

Memon, M. O., and Altman, A., "Wingtip Vortex Behavior in the vicinity of the Maximum Lift to Drag Ratio

Lift Condition", *54th AIAA Aerospace Sciences Meeting and Exhibit*, January 2016, San Diego, CA.

Wygnanski, F.; Champagne; Marasli, B., "On the Large-Scale Structures In Two-Dimensional, Small Deficit, Turbulent Wakes," *Journal of Fluid Mechanics*, Vol. 168, 1986, pp. 31-7.